1. Amelia KOSIOR-ROMANOWSKA[1], 2. Barbara STEFANIAK[1],3 Paweł TCHÓRZEWSKI, 4. Anna IWANICKA-MACIURA[1], 5. Dariusz WÓJCIK[1,2]

R&D Center Netrix S.A. Lublin, Poland (1), WSEI University (2)
ORCID: 1. 0009-0009-7050-0573; 2. 0000-0001-6555-8230;3 0000-0001-8344-8828, 4. 0009-0003-4617-2764, 5. 0000-0002-4200-3432

doi:10.15199/48.2025.01.36

Detecting lung diseases with electrical impedance tomography

***Abstract**. The article introduces a LETS vest designed to gather measurements for impedance tomography using damage excitation. It discusses the utilization of the IoT for impedance tomography. One of the key features will be disease diagnosis, specifically focusing on COPD in this context. The article presents classification models that can successfully differentiate between patients exhibiting COPD symptoms and healthy patients, achieving an impressive 98% accuracy rate.*

***Streszczenie.** Artykuł przedstawia kamizelkę LETS która zbiera pomiary dla tomografii impedancyjnej dla zadanego wzbudzenia. Przedstawiono IoT dla tomografii impedancyjnej. Jedną z funkcjonalności będzie rozpoznanie jednostek chorobowych, w tym przypadku POCHP. Przedstawiono modele klasyfikacji rozróżniające pacjenta z objawami POCHP, od pacjenta zdrowego ze skutecznością równą 98% (**Wykrywanie chorób płuc za pomocą elektrycznej tomografii impedancyjnej)**.*

Keywords: Electrical Impedance Tomography, Chronic Obstructive Pulmonary Disease, Finite Element Method.
Słowa kluczowe: Elektryczna Tomografia Impedancyjna, Przewlekła Obturacyjna CHoroba Płuc, Metoda Elementów Skończonych.

Introduction

Chronic obstructive pulmonary disease (COPD) is a disease with progressive, poorly reversible airflow through the breathing apparatus that arises from the rolling load in response to particulates, gases, and tobacco smoke [1]. The disease of the form is a progressive bronchial obstruction and occurs when there is an action with symptoms that worsen over time, i.e. shortness of breath, cough, and reduced exercise tolerance. Extrapulmonary changes often accompany this disease, which may adversely affect its course [2]. These are often cardiovascular diseases, weight loss and skeletal muscle weakness, nutritional disorders, or depression [3]. The severity classification (stage) of COPD is determined according to GOLD (Global Initiative for Chronic Obstructive Lung Disease) criteria based primarily on spirometry test results. There are 4 degrees of COPD severity: stage I (mild form), stage II (moderate form), stage III (severe form), and stage IV (very severe form combined with chronic respiratory failure) [4]. Chronic obstructive pulmonary disease is the fourth leading cause of death worldwide. In Poland, the number of patients is estimated at around 2 million [1]. The prognosis in severe COPD is serious and comparable to that in patients with advanced lung cancer. Various authors say the 5-year survival rate ranges from 26% to 50% [5]. The project's main objective is to create a mobile tomographic system for 3D imaging and spatial monitoring regions of interest. The system will consist of a mobile device enabling simultaneous recording of cardiac function and lung ventilation-related electrical potentials [6-7]. The future of medical diagnostics is devices that perform long-term patient monitoring - mobile devices that record a wide diagnostic spectrum to detect pathological syndromes. The answer to the needs of the medical market will be LETS - a mobile, tomographic 3D imaging and spatial monitoring system. The LETS system will enable monitoring of parameters based on changes in the node potential map (myocardial activity, blood flow, cardiac arrhythmias, atrioventricular conduction disturbances) and based on electrical tomography measurements (lung respiratory capacity, changes in lung impedance, relative electrical permeability) [8]. The LETS system, based on electrical tomography technology, will allow real-time imaging of lung ventilation while monitoring the heart's electrical activity by measuring electrocardiographic signals. This will allow monitoring of the condition of patients and support the diagnostic process in COPD [8].

Method

Electrical Impedance Tomography (EIT) [9-19] is the latest technology used in lung imaging. This method, based on the measurement of the electrical voltages on electrodes on surfaces, is characterized by high time resolution, allowing real-time tracking changes. It is a non-invasive method and practically devoid of side effects (no radiation and the need to transport the patient) [20]. This article describes the electrical tomography system with 32 active electrodes placed on vest LETS (Lung Electrical Tomography System) (Fig. 1).

Fig.1. LETS vest

The diagram shown in Fig. 2 depicts the basic elements of designing a medical electrical tomography monitoring platform with Internet of Things (IoT) devices and services. The UCU block represents a user-connected device: a personal device connected to the network (Laptop, Phone, Tablet) with the ability to connect to a wide area network (Internet).

The TS block executes web applications, in this case, using the Web Server Gateway Interface (WSGI). The MCU block is the microcontroller that is the interface to the IoT node's data acquisition and gateway system. In the MCU block, the tomographic application programming interface (TAPI) stores high-level programming functions to interact with the data acquisition process in the FTDAQ block.

The MCU triggers data acquisition. The configuration is loaded into FTDAQ using TAPI, and the experiment data can be read from FTDAQ memory to the MCU and directly stored in the TS database. The analog end block, AFE, contains components for digital control, mixed signal from analog to digital and digital to analog conversion, and signal conditioning for the transmitter and sensor parts. The SUM block denotes the system being measured and consists of an

electrode interface and a measuring system, which can be a test circuit, a tester of phantom material, organic tissue, or a test subject.

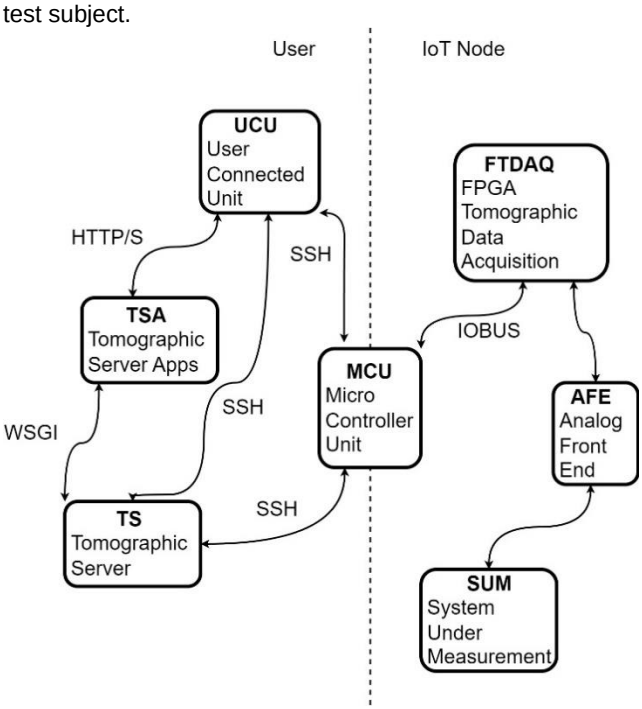

Fig.2. IoT platform for medical tomography

With the generation of digital re-configurable signal-mixing devices using FPGAs, fast, parallel, and coordinated data acquisition is a key advantage [21]. FPGAs are an essential component for real-time monitoring in tomography, given their prototyping capabilities and as an intermediary design for application-specific integrated circuits (ASICs). In the ASIC-based active electrode system from [22], the central port is controlled by an FPGA. Another application of the FPGA is accelerating computational procedures. A semi-parallel potential and current excitation emitter have been developed using the FPGA as a hardware acceleration [23] for FFT calculations and signal filtering.

Further applications may include online nonlinear analysis, such as mutual information [24], acceleration of reconstruction using iterative algorithms, and artificial intelligence algorithms, such as neural networks.

Modelling the measurement process

We consider a model of the male torso based on computer tomography (CT) images. Following the segmentation process to isolate the torso and lungs from the background, our next step involves generating a mesh composed of tetrahedral elements. We intend to showcase a comprehensive outline of the mesh generation procedure and the subsequent data processing stages (Fig. 3).

The first step of our algorithm is to load a 3D image represented as a 3D matrix composed of 0, 1, and 2, where each 0 means an element outside the field of view, 1 indicates a human torso, and 2 - human lungs. The next step is the preparation of a mesh made of tetrahedrons. It is necessary to create a grid composed of voxels, then find the voxels located in the field of view (represented as 1 and 2 in the 3D matrix) (Fig. 4), and finally create a tetrahedrons mesh (Fig. 5). Then, using a vest (Fig.1.), the electrodes were applied to the model at levels 0.0 and -0.2 as 16 equidistant points. In this way, we created a three-dimensional mesh of the human torso and lungs consisting of 1617066 tetrahedral elements with two bands of electrodes (Fig.6).

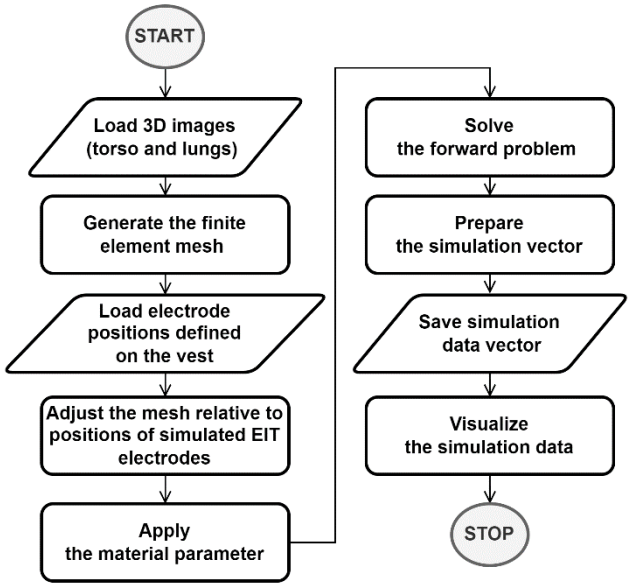

Fig.3. Block diagram of the EIT data frame simulation process

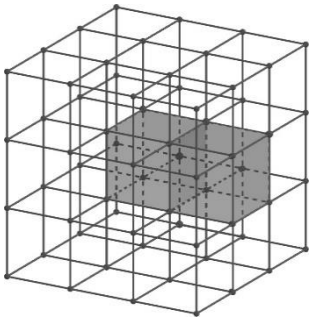

Fig.4. Voxels located in the field of view

In the model, as an application of the material parameter, we considered three coefficients: 0.14, β equation (3), 0.35 corresponding respectively to the healthy lung area, lungs with COPD-related changes, and the area outside the lungs. The next step of the algorithm is to solve a forward problem. To solve the forward problem, we start with the equation:

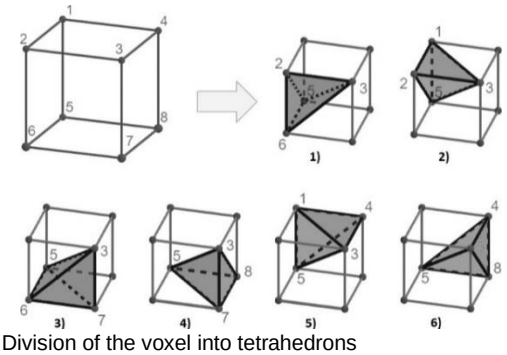

Fig.5. Division of the voxel into tetrahedrons

(1)

$$E[\phi] = \int\int\int_{\Pi} \sigma \, ||\nabla\phi||^2 d\pi + \sum_{l} \frac{1}{z_l} \int\int_{\mathrm{L}} (\phi - U_l)^2 d\omega$$

where σ- conductivity, ∇- gradient, ϕ-potential, π- element volume L – field of the electrode, U_l – potential on l – electrode.

With point electrodes in the model, the equation above is simplified to

(2) $$E(\phi) = \int\int\int_{\Pi} \sigma \, ||\nabla\phi(v)||^2 d\pi$$

We employ the Finite Element Method (FEM) with tetrahedral elements to acquire measurements.

We begin with 81 observations to prepare the neural network dataset. The first observation comes from a model simulating a healthy object (Fig. 6.), while the remaining observations are from objects with an illness (Fig.7. diseased lungs are shown in a different color). Figures were limited to several horizontal cross-sections of the torso considering the two levels of electrodes (electrodes marked with points) and lung lumps. The illnesses in these objects are introduced using the following formula
(3)

$$\mathrm{Img}[\mathrm{indCOPD}] = \beta = 0.14\,\alpha + 0.35(1-\alpha), \alpha \in [0.1, 0.9]$$

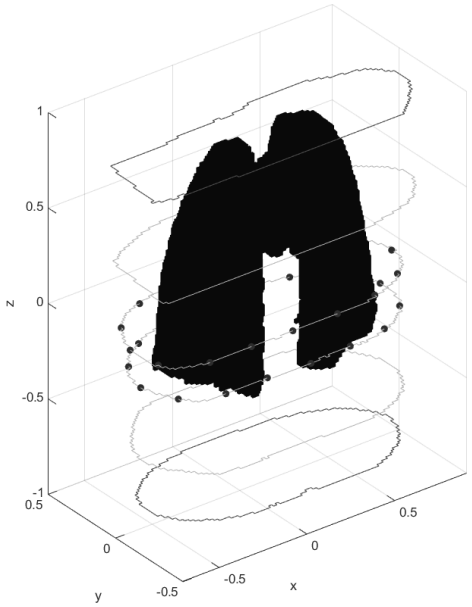

Fig. 6. Visualization of healthy lungs

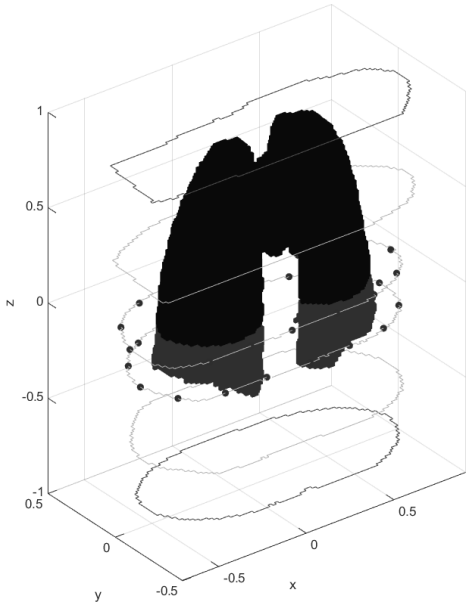

Fig. 7. Visualization of unhealthy lungs

The measurements were simulated using polar excitation and neighboring measurements. For 32 electrodes, we get 448 measurements. To achieve 10,040 observations, we introduced random normal noise with a mean of 0 and a standard deviation of 0.8.

Classification

The dataset had 5001 rows describing healthy and 5040 lungs with simulated liquid. Variables representing observations of unhealthy lungs had greater variability than variables describing healthy lung observations. The difference above positively affected the separability of data from both classes. The boxplot and results of Kruskal-Wallis statistical tests for the selected variable are presented below (Fig 8).

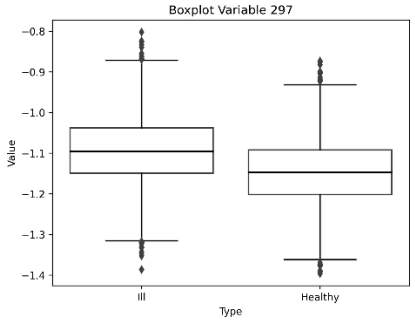

Fig. 8. Differences between the classes on 297 variables

Based on the results, we observe fundamental differences between the classes, positively impacting the classification process.

Predictive models were constructed based on the generated observations. The training set contained 9541 observations, while the test set included 500 observations. The study used three algorithms: logistic regression, gradient boosting, and naive Bayesian classifier using default parameters. The obtained predictive results proved satisfactory, as logistic regression and gradient boosting achieved a classification efficiency close to 100 %. In contrast, the efficiency of the naive Bayesian classifier has already settled at 97%. After detailed testing, it was found that only the boosting algorithm did not make errors on real observations. Hence it was considered the optimal solution. The confusion Matrices for each algorithm are as follows (Fig 9 - 11).

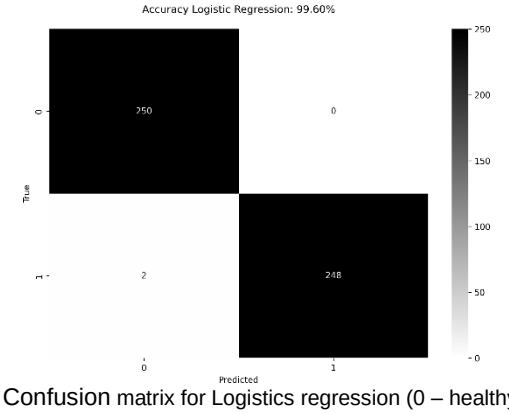

Fig. 9. Confusion matrix for Logistics regression (0 – healthy, 1 – unhealthy lungs)

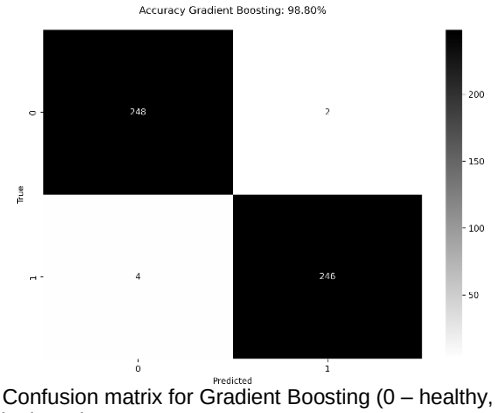

Fig. 10 Confusion matrix for Gradient Boosting (0 – healthy,1 - unhealthy lungs)

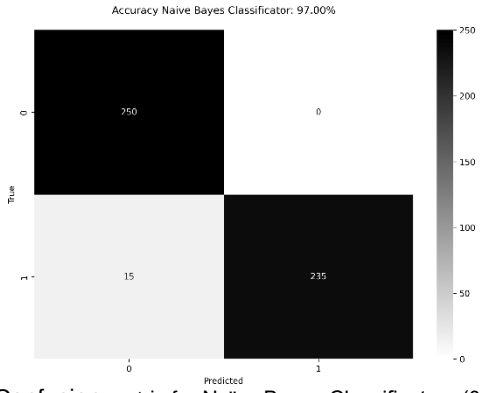

Fig. 11 Confusion matrix for Naïve Bayes Classificatory (0 – healthy, 1 – unhealthy lungs)

Conclusions

This article presents an EIT system designed for biomedical applications. The system is aimed at non-invasive imaging of the lungs through electrical tomography, a method that utilizes electrical currents to examine unknown physical objects. The article presents a numerical model of the lungs and discusses the results of numerical simulations conducted on healthy lungs and lungs displaying signs of pathological Chronic Obstructive Pulmonary Disease (COPD). The finite element method was employed to solve the forward problem, and calculations were conducted on the defined model to establish data classification models. The article also outlines the Internet of Things architecture implemented for the LETS (Lung Electrical Tomography System) vest. The hardware solution is based on an FPGA chip. The overall system represents a portable solution for capturing the electrical potential of the lungs, serving as the LETS vest system for innovative imaging and signal analysis.

***Authors**: dr Amelia Kosior-Romanowska, M.Sc., Research and Development Center Netrix S.A E-mail: amelia.kosior@netrix.com.pl mgr Barbara Stefaniak, M.Sc., Research and Development Center Netrix S.A E-mail: barbara.stefaniak@netrix.com.pl. mgr Paweł Tchórzewski, M.Sc., Research and Development Center Netrix S.A E-mail: pawel.tchorzewski@netrix.com.pl. dr Anna Iwanicka-Miciura, M.Sc., Research and Development Center Netrix S.A E-mail: anna.miciura@netrix.com.pl; dr inż. Dariusz Wójcik, Akademia WSEI, Wydział transportu i informatyki, ul. Projektowa 4, 20-209 Lublin, E-mail: dariusz.wojcik@wsei.lublin.pl*

REFERENCES

[1] Jassem E., Górecka D., Severe and terminal chronic obstructive pulmonary disease, *Pneumonol. Alergol. Pol.*, 77 (2009), No. 4, 411- 416.

[2] Gutknecht P., Trzeciak B.G., Siebert J., Knowledge of the patients about chronic obstructive pulmonary disease, *Family Medicine & Primary Care Review*, 16 (2014), No. 2, 99 - 100.

[3] Chazan R., New therapeutic possibilities in COPD, *Pneumonol. Alergol. Pol.* (2013), No. 81, 154 -161.

[4] Liebhart J., Natural history of the patient's disease course with COPD – from diagnosis to distress, *Medycyna po Dyplomie*, 20 (2011), No. 5 (182), 56-60.

[5] Rizkallah J., Man S.F.P., Sin D.D., Prevalence of pulmonary embolism in acute exacerbations of chronic obstructive pulmonary disease: a systematic review and meta-analysis, *Chest* (2009), No. 135, 786-793.

[6] Searle A., Kirkup L., A direct comparison of wet, dry and insulating bioelectric recording electrodes, *Physiol Meas*. (2000), 21(2):271-83.

[7] Yapici M. K., Alkhidir T., Samad Y. A., Liao K., Graphene-clad textile electrodes for electrocardiogram monitoring, *Sensors and Actuators B: Chemical*, 221 (2015), 1469 – 1474.

[8] Rymarczyk T., Nita P., Véjar A., Stefaniak B., Sikora J., Electrical tomography system for Innovative Imaging and Signal Analysis, *Przegląd Elektrotechniczny* 7, R. 95 NR 6 (2019), 133-136

[9] Gnaś, D., Adamkiewicz, P., Indoor localization system using UWB, Informatyka, Automatyka, Pomiary W Gospodarce I Ochronie Środowiska, 12 (2022), No. 1, 15-19.

[10] Koulountzios P., Aghajanian S., Rymarczyk T., Koiranen T., Soleimani M., An Ultrasound Tomography Method for Monitoring CO2 Capture Process Involving Stirring and CaCO3 Precipitation, Sensors, 21 (2021), No. 21, 6995.

[11] Kłosowski G, Rymarczyk T, Niderla K, Kulisz M, Skowron Ł, Soleimani M., Using an LSTM network to monitor industrial reactors using electrical capacitance and impedance tomography – a hybrid approach. Eksploatacja i Niezawodnosc – Maintenance and Reliability, 25 (2023), No. 1, 11.

[12] Kłosowski G., Rymarczyk T., Kania K., Świć A., Cieplak T., Maintenance of industrial reactors supported by deep learning driven ultrasound tomography, Eksploatacja i Niezawodnosc – Maintenance and Reliability; 22 (2020), No 1, 138–147.

[13] Styła, M., Adamkiewicz, P., Optimisation of commercial building management processes using user behaviour analysis systems supported by computational intelligence and RTI, Informatyka, Automatyka, Pomiary W Gospodarce I Ochronie Środowiska, 12 (2022), No 1, 28-35.

[14] Kropidłowska P., Irzmańska E. Korzeniewska E., Tomczyk M., Jurczyk-Kowalska M., Evaluation of laser texturing in fabricating cut-resistant surfaces for protective gloves, Textile Research Journal, 93 (2023), No. 9-10), 1917–1927.

[15] Pawłowski S., Plewako J., Korzeniewska E., Field Modeling of the Influence of Defects Caused by Bending of Conductive Textronic Layers on Their Electrical Conductivity, Sensors, 23 (2023), No. 3, 1487.

[16] Rymarczyk T., Kłosowski G., Hoła A., Hoła J., Sikora J., Tchórzewski P., Skowron Ł., Historical Buildings Dampness Analysis Using Electrical Tomography and Machine Learning Algorithms, Energies, 14 (2021), No. 5, 1307.

[17] Kłosowski G., Rymarczyk T., Niderla K., Rzemieniak M., Dmowski A., Maj M., Comparison of Machine Learning Methods for Image Reconstruction Using the LSTM Classifier in Industrial Electrical Tomography, Energies 2021, 14 (2021), No. 21, 7269.

[18] Rymarczyk T., Kłosowski G., Hoła A., Sikora J., Tchórzewski P., Skowron Ł., Optimising the Use of Machine Learning Algorithms in Electrical Tomography of Building Walls: Pixel Oriented Ensemble Approach, Measurement, 188 (2022), 110581.

[19] Koulountzios P., Rymarczyk T., Soleimani M., A triple-modality ultrasound computed tomography based on full-waveform data for industrial processes, IEEE Sensors Journal, 21 (2021), No. 18, 20896-20909.

[20] Białka Sz., Maja Copik M., Rybczyk K., Misiołek H., Electrical impedance tomography for diagnosis and monitoring of pulmonary function disorders in the intensive care unit - case report and review of literature, *Anestezjologia Intensywna Terapia,* 49 (2017), No. 3, 228-233.

[21] Mierzejewski K., Véjar A., A Platform for Joint Analysis of Biosignals Ensembles in Real-Time Using Fpga, *Acta Bio-Optica et Informatica Medica. Inżynieria Biomedyczna,* 22 (2016), No. 4, 253–60.

[22] Wu Y., Jiang D., Bardill A., de Gelidi S., Bayford R.H., & Demosthenous A., A High Frame Rate Wearable EIT System Using Active Electrode ASICs for Lung Respiration and Heart Rate Monitoring. *IEEE Transactions on Circuits and Systems I: Regular Papers*, 65 (2018), 3810-3820.

[23] Khan S., Manwaring P.K., Borsic A., Halter R.J. FPGA-Based Voltage and Current Dual Drive System for High Frame Rate Electrical Impedance Tomography, IEEE *Transactions on Medical Imaging*, 34 (2015), 888-901.

[24] Véjar A., Rymarczyk T., Paprzycki P., Mutual Information and Delay Embeddings in Polysomnography Studies*, International Interdisciplinary PhD Workshop (IIPhDW)*, (2019), 89-94.